

# Edge states and the integer quantum Hall effect of spin-chiral ferromagnetic kagomé lattice with a general spin coupling

Zhigang Wang and Ping Zhang

*Institute of Applied Physics and Computational Mathematics, P.O. Box 8009, Beijing 100088, P.R. China*

The chiral edge states and the quantized Hall conductance (QHC) in the two-dimensional kagomé lattice with spin anisotropies included in a general Hund's coupling region are studied. This kagomé lattice system is periodic in the  $x$  direction but has two edges in the  $y$  direction. Numerical results show that the strength of the Hund's coupling, as well as the spin chirality, affects the edge states and the corresponding QHC. Within the topological edge theory, we give the expression of the QHC with the winding number of the chiral edge states on the Riemann surface. This expression is also compared with that within the topological bulk theory and they are found to keep consistent with each other.

PACS numbers: 73.43.-f, 73.43.Cd, 71.27.+a

## I. INTRODUCTION

The quantum Hall effect (QHE), in which the Hall conductance (HC)  $\sigma_{xy}$  is quantized with extremely high accuracy, is a typical realization of topological effects in condensed matter physics [1]. The topological aspect of the QHE with a periodic potential was first discussed by Thouless, Kohmoto, Nightingale, and den Nijs [2]. In their work, the HC is given by the Chern number [3] over the magnetic Brillouin zone, which is a topological expression by the bulk state. Later Hatsugai [4] suggested that the HC can be given by another topological quantity, i.e., the "winding number" of the edge states on the complex-energy surface which is generally a high-genus Riemann surface. To distinguish them, we call the former "the bulk theory" and the latter "the edge theory". The two topological expressions for the HC, which look quite different, actually give the same integer number.

A recent established recognition points out that the conventional QHE originates from the non-local effect provided by the external magnetic field, more exactly speaking, by the vector potential that describes the magnetic field. That means a non-zero vector potential, for example, which can be provided by spin-orbit interaction or by spin chirality, will induce the QHE even if the external magnetic field vanishes. This type of QHE can be called "the anomalous QHE" [5, 6, 7]. Since Haldane performed the famous "Haldane model" in his pioneering work [5] in 1988, the anomalous QHE in spin-orbit coupled [8, 9, 10] or spin-chiral ferromagnetic systems [11, 12, 13, 14] has been a hot topic in condensed matter physics. Based on the tight-binding two-dimensional (2D) graphite model [15], Haldane model includes the next-nearest neighboring interaction and a periodic local magnetic-flux density, which breaks time-reversal invariance and creates a chirality. However, because the introduction of local flux is technically difficult, it is not so easy to realize Haldane model in real materials. Another typical spin-chiral system is the ferromagnetic system, which is represented by pyrochlore compounds  $R_2\text{Mo}_2\text{O}_7$  ( $R=\text{Nd, Sm, Gd}$ ), in which the spin configuration is non-

coplanar and the spin chirality appears. Ohgushi et al. [6] have first pointed out that the chiral spin state can be realized by the introduction of spin anisotropy in an *ordered* spin system on the 2D kagomé lattice, which is the cross section of the pyrochlore lattice perpendicular to the (1, 1, 1) direction [16]. In this case, it has been shown in the topological bulk theory [6, 17] that the presence of chiral spin state may induce gauge-invariant nonzero Chern number, thus resulting in a QHE in insulating state. However, as stressed by Halperin [18], this gauge invariance has a relation with the edge states which are localized near the sample boundaries. Recently we reinvestigated the kagomé lattice with boundaries. Using the topological edge theory established by Hatsugai in the last decade [4], we interpreted the quantized Hall conductance (QHC) in insulating state with the winding number of the edge states on the complex-energy surface [19].

In the above-mentioned theoretical works [6, 17, 19] on the 2D kagomé lattice, a very important limit has been used. That is the hopping electron spins are aligned with localized spins at each site of the lattices, which is also called the "infinite (*strong*) Hund's coupling limit". However, the latest detailed experiments on the pyrochlores [20] showed that the spin-chiral mechanism *alone* can not explain the anomalous transport phenomena in these systems. So in this paper we study the 2D kagomé lattice with boundaries in a general Hund's coupling region, especially in the weak coupling region [21]. We find that the edge states and QHC are not only affected by the spin chirality, but also affected by the strength of the Hund's coupling. Varying the spin chirality and the strength of the Hund's coupling, two different types of phenomena are obtained. In one case that the strength of the Hund's coupling is larger than its critical value (see [22] or Sec. III), there are only two edge-state energies in each bulk energy gap. With the help of the topological edge theory, we obtain that the corresponding HC is quantized as  $\sigma_{xy} = \pm \frac{e^2}{h}$  in insulating state. However, in another case that the Hund's coupling strength is smaller than its critical value, there are *possibly* four edge-state energies in

some one bulk gap. In this case, within the topological edge theory, we obtain that the corresponding HC is quantized as  $\sigma_{xy} = \pm 2 \frac{e^2}{h}$  in this insulating state, which can not occur in the strong Hund's coupling case. We also make a comparison between these results and those in the bulk theory [22], and find that they keep consistent with each other.

This paper is organized as the following. In sec. II, we introduce the tight-binding model of the 2D kagomé lattice with boundaries along the  $y$  direction and obtain the eigenvalue equations for sites. We also write out the Hamiltonian of the 2D kagomé lattice without boundaries in the reciprocal space in this section. Because the analytical derivation is very difficult, then in sec. III, we numerically calculate the energy spectrum. Using the characters of the edge-state energies in the spectrum, we study the QHE within the topological edge theory. As comparison, we also recalculate the HC in the infinite system in this section. Finally we make a conclusion in the last section.

## II. MODEL

We consider the double-exchange ferromagnet kagomé lattice schematically shown in Fig. 1(a). The triangle is one face of the tetrahedron. Here we consider a pure spin model with anisotropic Dzyaloshinskii-Moriya interactions on a kagomé lattice. It consists of an umbrella of three spins per unit cell of the kagomé lattice. Each umbrella can be described by the spherical coordinates of the three spins  $(\pi/6, \theta)$ ,  $(5\pi/6, \theta)$ , and  $(-\pi/2, \theta)$ , as shown in Fig. 1(b). The angle  $\theta$  ranges from 0 to  $\pi$ .

The tight-binding model of the 2D kagomé system can be written as the following [22]

$$H = \sum_{\langle i,j \rangle, \sigma} t_{ij} \left( c_{i\sigma}^\dagger c_{j\sigma} + \text{H.c.} \right) - J_0 \sum_{i, \alpha, \beta} c_{i\alpha}^\dagger (\sigma_{\alpha\beta} \cdot \mathbf{n}_i) c_{i\beta}, \quad (1)$$

where  $t_{ij}$  is the hopping integral between two neighboring sites  $i$  and  $j$ ;  $c_{i\sigma}^\dagger$  and  $c_{i\sigma}$  are the creation and annihilation operators of an electron with spin  $\sigma$  on the site  $i$ .  $J_0$  is the effective coupling constant to each local moment  $\mathbf{S}_i$ , and these moments are treated below as classical variables.  $\mathbf{n}_i$  is a unit vector collinear with the local moment  $\mathbf{S}_i$ .  $\sigma_{\alpha\beta}$  are the Pauli matrices. In the following we change notation  $i \rightarrow (lms)$ , where  $(lm)$  labels the kagomé unit cell and  $s$  denote the sites A, B and C in this cell. The size of the unit cell is set to be unit throughout this paper. This Hamiltonian has already been discussed in the infinite Hund's coupling limit  $J_0 \rightarrow \infty$  in Refs. [6, 17, 19]. In this limit the two  $\sigma = \uparrow, \downarrow$  bands are infinitely split and the model describes a fully polarized electron subject to a modulation of a fictitious magnetic field, corresponding to the molecular field associated with the magnetic texture.

Now we suppose that the system is periodic in the  $x$  direction but has two edges in the  $y$  direction (see Fig.

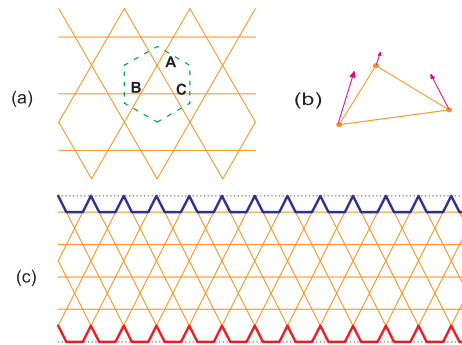


FIG. 1: (Color online) (a) 2D spin-chiral ferromagnetic kagomé lattice. The dashed line represents the Wigner-Seitz unit cell, which contains three independent sites (A, B, C). (b) The umbrella structure on the triangular cell of the 2D kagomé lattice. (c) The 2D kagomé lattice system with boundaries along the  $y$  direction. The bold lines are correspond to the down and up edges, respectively.

1(c)). Since the system is periodic in the  $x$  direction, we can use a momentum representation of the electron operator

$$c_{(lms\sigma)} = \frac{1}{\sqrt{L_x}} \sum_{k_x} e^{ik_x X_{(lms)}} \gamma_{lms\sigma}(k_x), \quad (2)$$

where  $\mathbf{R}_{(lms)} = (X_{(lms)}, Y_{(lms)})$  are the coordinate of the site  $s$  in the unit cell  $(lm)$  and  $k_x$  is the momentum along the  $x$  direction. Let us consider the one-particle state  $|\Psi(k_x)\rangle = \sum_{m,s\sigma} \Psi_{ms}(k_x) \gamma_{ms}^\dagger(k_x) |0\rangle$ . Inserting it into the Schrödinger equation  $H|\Psi\rangle = E|\Psi\rangle$ , we can easily obtain the following three eigenvalue equations for sites A, B, and C,

$$\begin{aligned} E\Psi_{mA\sigma} &= e^{-i\frac{k_x}{4}} \Psi_{mB\sigma} + e^{i\frac{k_x}{4}} \Psi_{m+1B\sigma} \\ &\quad + e^{i\frac{k_x}{4}} \Psi_{mC\sigma} + e^{-i\frac{k_x}{4}} \Psi_{m+1C\sigma} \\ &\quad - \sigma J_0 \cos\theta \Psi_{mA\sigma} + i\bar{\sigma} J_0 \sin\theta \Psi_{mA\bar{\sigma}}, \\ E\Psi_{mB\sigma} &= e^{i\frac{k_x}{4}} \Psi_{mA\sigma} + e^{-i\frac{k_x}{4}} \Psi_{m-1A\sigma} \\ &\quad + 2 \cos(k_x/2) \Psi_{mC\sigma} \\ &\quad - \sigma J_0 \cos\theta \Psi_{mB\sigma} - J_0 e^{i\bar{\sigma}\frac{\pi}{6}} \sin\theta \Psi_{mB\bar{\sigma}}, \\ E\Psi_{mC\sigma} &= e^{-i\frac{k_x}{4}} \Psi_{mA\sigma} + e^{i\frac{k_x}{4}} \Psi_{m-1A\sigma} \\ &\quad + 2 \cos(k_x/2) \Psi_{mB\sigma} \\ &\quad - \sigma J_0 \cos\theta \Psi_{mC\sigma} - J_0 e^{i\bar{\sigma}\frac{5\pi}{6}} \sin\theta \Psi_{mC\bar{\sigma}}. \end{aligned} \quad (3)$$

Here we set  $t_{ij}=1$  as the energy unit,  $\sigma = \pm 1$  denotes the spin up and down, respectively.  $\bar{\sigma} = -\sigma$ . Eliminating the B- and C-sublattice sites, one can obtain a difference equation for  $\Psi_{A\sigma}$ , which is the famous Harper equation [23]. Because the expression of the Harper equation is too sophisticated to perform a help in analytical resolving the edge states, we turn to make a numerical calculation and analysis from Eq. (3).

If the system is also periodic in the  $y$  direction, the Hamiltonian can be rewritten in the reciprocal space. We use the momentum representation of the electron operator  $c_{(lms\sigma)} = \frac{1}{\sqrt{L_x L_y}} \sum_{\mathbf{k}} e^{i\mathbf{k}\cdot\mathbf{R}_{(lms)}} \gamma_{s\sigma}(\mathbf{k})$ . Inserting the

one-particle state  $|\Psi(\mathbf{k})\rangle = \sum_{s\sigma} \Psi_{s\sigma}(\mathbf{k}) \gamma_{s\sigma}^\dagger(\mathbf{k}) |0\rangle$  into the Schrödinger equation  $H|\Psi\rangle = E|\Psi\rangle$ , we can easily obtain the Hamiltonian in the reciprocal space  $H(\mathbf{k})$ , which is given by

$$H(\mathbf{k}) = \begin{pmatrix} -J_0 \cos \theta & p_{\mathbf{k}}^1 & p_{\mathbf{k}}^3 & iJ_0 \sin \theta & 0 & 0 \\ p_{\mathbf{k}}^1 & -J_0 \cos \theta & p_{\mathbf{k}}^2 & 0 & -J_0 e^{-i\frac{\pi}{6}} \sin \theta & 0 \\ p_{\mathbf{k}}^3 & p_{\mathbf{k}}^2 & -J_0 \cos \theta & 0 & 0 & -J_0 e^{-i\frac{5\pi}{6}} \sin \theta \\ -iJ_0 \sin \theta & 0 & 0 & J_0 \cos \theta & p_{\mathbf{k}}^1 & p_{\mathbf{k}}^3 \\ 0 & -J_0 e^{i\frac{\pi}{6}} \sin \theta & 0 & p_{\mathbf{k}}^1 & J_0 \cos \theta & p_{\mathbf{k}}^2 \\ 0 & 0 & -J_0 e^{i\frac{5\pi}{6}} \sin \theta & p_{\mathbf{k}}^3 & p_{\mathbf{k}}^2 & J_0 \cos \theta \end{pmatrix}, \quad (4)$$

where  $p_{\mathbf{k}}^1 = 2 \cos(k_x/4 + \sqrt{3}k_y/4)$ ,  $p_{\mathbf{k}}^2 = 2 \cos(k_x/2)$  and  $p_{\mathbf{k}}^3 = 2 \cos(-k_x/4 + \sqrt{3}k_y/4)$ .

### III. EDGE STATES AND THE HALL CONDUCTANCE

Before investigating the chiral edge states and QHC of the 2D kagomé lattice with boundaries, we simply discuss the energy structures of this system with different exchange interaction  $J_0$ . Firstly in the absence of the exchange interaction, i.e.,  $J_0=0$ , Eq. (2) becomes to be independent of both the spin index  $\sigma$  and the chiral parameter  $\theta$ . In this case the two  $\sigma=\uparrow, \downarrow$  bands are completely degenerate and there are only three bulk energy bands, between which there are no bulk energy gaps, as shown in Fig. 2. From Fig. 2, one can see that the lower energy band becomes dispersionless ( $E=-2$ ), which reflects the fact that the 2D kagomé lattice is a line graph of the honeycomb structure [24]. This flat band touches at  $k_x=0$  with the middle band, while the middle band touches at  $k_x=\frac{2\pi}{3}, \frac{4\pi}{3}$  with the upper band.

In the existence of exchange interaction, i.e.,  $J_0 \neq 0$ , the energy spectrum splits into two parts due to the spin-dependent potential. For very large values of  $J_0$ , the spectrum is divided into two groups of three bands, which is the infinite Hund's coupling case studied in Ref. [19]. For nonzero but not too large values of  $J_0$ , we numerically calculate the energy spectrum and find that there are main two different phenomena for QHE happening. The critical value of the exchange interaction  $J_c$  depends on the chiral parameter  $\theta$ . In the topological bulk theory [22], this critical value is analytically obtained, which reads as

$$J_c(\theta) = \pm 2/\sqrt{1+3\cos^2\theta}. \quad (5)$$

Although in the present model with boundaries, the critical value  $J_c(\theta)$  can not be analytically obtained, the numerical calculations tell us that the above expression of  $J_c(\theta)$  [Eq. (5)] is also approximately valid for the present

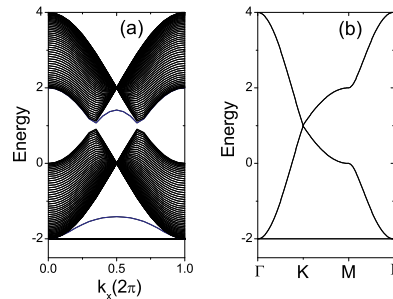


FIG. 2: (Color online) The energy spectrums of the 2D kagomé lattice (a) with boundaries along the  $y$  direction and (b) without boundaries. In both figures, the exchange interaction  $J_0=0$ . There are only three energy bands and there are *no* bulk gaps between them. The lower band is flat, which reflects that the 2D kagomé lattice is a line graph of the honeycomb structure. In Fig. 2(a), the blue lines denote the up-edge-state energies.

model. In the following, we investigate the HC in both cases.

#### A. Case I: $J_0 < J_c$

In the following we study the QHE of 2D kagomé system with boundaries in both cases. First, we investigate the case  $J_0 < J_c$ . As an example, we choose the fixed chiral parameter as  $\theta=\pi/3$ , and the exchange interaction as  $J_0=1$  ( $J_c=4/\sqrt{7} \approx 1.51$ ). The number of site A (or B, C) in the  $y$  direction is chosen to be  $L_y=31$ . By numerical calculating Eq. (3), we draw in Fig. 3(a) the energy spectrum in this case. From this figure, one can clearly see that the two groups of three bulk bands are not completely divided (i.e., there is no Mott gap) and there are two bulk gaps appearing. The range of the lower energy gap is between  $-2.68$  and  $-2.6$ , and that of the higher energy gap is between  $1.1$  and  $1.4$ , which are enlarged in Figs. 3(b) and 3(c), respectively.

In the topological edge theory [4], when the Fermi energy lies in one energy gap, the HC of the system is given by the winding number of the edge states  $I$ ,  $\sigma_{xy}^{\text{edge}} = -\frac{e^2}{h}I$ . The winding number is given by the number of the intersection between the canonical loop  $\alpha_i$  on the Riemann surface (the complex energy surface) and the trace of the edge-state energy  $\mu_i$ . Although in present model, the Riemann surface is more sophisticated than that in the infinite Hund's coupling case [19], we can follow the analysis in the previous work [19] to discuss the winding number of the edge state. Because the analytical process is same as that in the strong Hund's coupling case, here we only present the results as the following:

The winding number of the edge states is given by the sum of the intersection number between the Fermi energy  $\epsilon_f$  and the energies of the down (or up) edge state in one period. The down (or up) edge states refer to the eigenstates which are localized near the down (or) up boundaries of the sample. The intersection number is obtained as: In the left neighboring of the intersection, if the down-edge-state energy is connected with the lower energy band, or the up-edge-state energy is connected with the upper energy band, the intersection number is given by “+1”. If not, it is given by “-1”.

Now with the above results, we investigate the HC of the system. From Fig. 3(b), one can see that when the Fermi energy  $\epsilon_f$  lies in the lower gap (LG), there is only one intersection between  $\epsilon_f$  and the down edge-state energy, which is labeled as A in Fig. 3(b). In the left neighboring of the intersection A, the down edge-state energy is connected with the lower band. So the winding number of the edge state is  $I_1 = +1$ . With the same method, one can find in Fig. 3(c) there are four edge-state energies lie in the higher gap (HG). When the Fermi energy  $\epsilon_f$  lies in the HG, there are *two* intersections (labeled as B and C in Fig. 3(b)) between  $\epsilon_f$  and the down edge-state energies. Because in the left neighboring of the intersections, the down edge-state energies are connected with the lower band, we can obtain that the winding number of the edge states is  $I_2 = +2$ . According to the topological edge theory, we can get the QHC as

$$\sigma_{xy}^{\text{edge}} = \begin{cases} -\frac{e^2}{h}I_1 = -\frac{e^2}{h}, & \epsilon_f \in \text{the lower gap} \\ -\frac{e^2}{h}I_2 = -2\frac{e^2}{h}, & \epsilon_f \in \text{the higher gap} \end{cases} \quad (6)$$

To check the above results, we recalculate the energy spectrum and the HC of the 2D kagomé lattice *without* boundaries within the topological bulk theory. This system has been studied by Taillefer et al. [22]. In the bulk theory, when the Fermi energy  $\epsilon_f$  lies in the energy gap, the HC of the system in units of  $e^2/h$  is given by the sum of the Chern numbers of all the occupied energy bands [3]:  $\sigma_{xy}^{\text{bulk}} = \frac{e^2}{h} \sum_{n=1}^{\text{occu}} C_n$ . The Chern number of the  $n$ -th band is defined as  $C_n = \frac{1}{2\pi} \int \Omega_{\mathbf{n}\mathbf{k}}^z d^2\mathbf{k}$ , where  $\Omega_{\mathbf{n}\mathbf{k}}^z = \nabla_{\mathbf{k}} \times \mathbf{A}_{\mathbf{n}\mathbf{k}}$ , and  $\mathbf{A}_{\mathbf{n}\mathbf{k}} = -i \langle u_{\mathbf{n}\mathbf{k}} | \nabla u_{\mathbf{n}\mathbf{k}} \rangle$  is the geometric vector potential. With the Hamiltonian in the momentum representation  $H(\mathbf{k})$  [Eq. (4)], after a straightforward numerical calculation, one can obtain the Chern

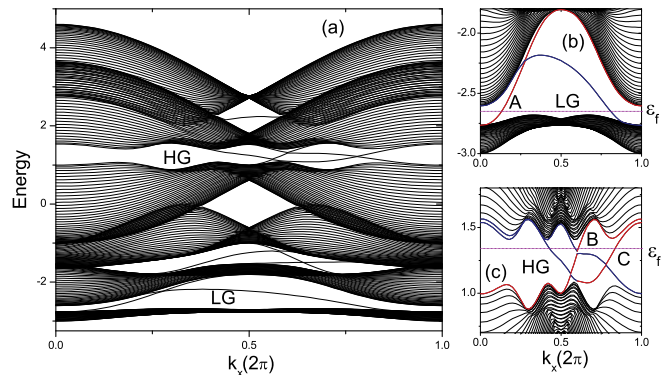


FIG. 3: (Color online) (a) The energy spectrum of 2D kagomé lattice with edges along the  $y$  direction. The parameters are chosen as  $J_0=1$ ,  $\theta=\pi/3$ . The shaded areas are energy bands and the lines are the spectrum of the edge states. In this case, there is no Mott gap and there are two energy gaps, which are enlarged in (b) and (c). In (b) and (c), the red and blue lines correspond to the down and up edge-state energies, respectively.

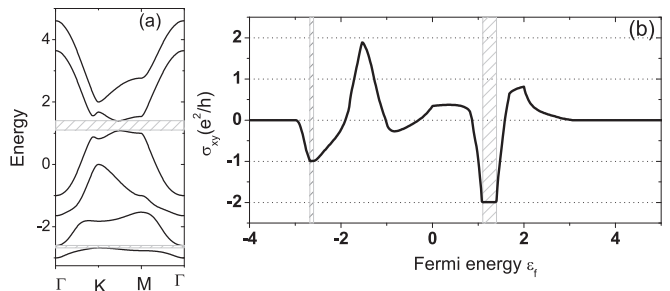


FIG. 4: (a) The energy spectrum of the 2D kagomé lattice without edges. The parameters are same as that in Fig. 3. (b) The Hall conductance  $\sigma_{xy}$  of this system as a function of the Fermi energy  $\epsilon_f$  at the temperature  $T=0$ . In both figures, the shaded areas are the bulk energy gaps.

numbers are  $-1, 3, -2, -2, 3, -1$  from the lowest to the topmost band. So, when the Fermi energy lies in the LG,  $\sigma_{xy}^{\text{bulk}} = \frac{e^2}{h}C_1 = -\frac{e^2}{h}$ ; when the Fermi energy lies in the HG,  $\sigma_{xy}^{\text{bulk}} = \frac{e^2}{h} \sum_{n=1}^4 C_n = -2\frac{e^2}{h}$ . Compare with Eq. (6), one obtain that  $\sigma_{xy}^{\text{edge}} = \sigma_{xy}^{\text{bulk}}$ . In Fig. 4(b), we plot the HC as a function of the Fermi energy  $\epsilon_f$  using the finite-temperature formula  $\sigma_{xy} = \frac{e^2}{h} \sum_n \frac{1}{2\pi} \int f_{\mathbf{n}\mathbf{k}} \Omega_{\mathbf{n}\mathbf{k}}^z d^2\mathbf{k}$ , where  $f_{\mathbf{n}\mathbf{k}}$  is the Fermi distribution function. From this figure, one can see that when the system is in the insulating state, the HC is quantized. In the LG, the conductance is  $\sigma_{xy} = -\frac{e^2}{h}$ , and in the HG, the conductance is  $\sigma_{xy} = -2\frac{e^2}{h}$ . Fig. 4(a) plots the energy spectrum of the system without boundaries.

Note that in the strong Hund's coupling limit [19], the non-zero QHC only takes two values,  $\pm \frac{e^2}{h}$ . So this is a novel result that the HC can take the value  $\pm 2\frac{e^2}{h}$  in the

weak Hund's coupling.

### B. Case II: $J_0 > J_c$

Then we consider the other case, in which  $J_0 > J_c$ . As an example, we choose the fixed chiral parameter  $\theta = \pi/3$  and the exchange interaction  $J_0 = 2$ . The number of sites A (or B, C) in the  $y$  direction is also chosen to be  $L_y = 31$ . With Eq. (3), we plot in Fig. 5(a) the energy spectrum of the 2D kagomé lattice with boundaries. From Fig. 5(a), one can find that there are four gaps in this case. We call them G-I, G-II, G-III (which is the Mott gap), and G-IV corresponding to that between  $-3.54$  and  $-3.36$ , between  $-2.0$  and  $-1.65$ , between  $-1$  and  $0$ , and between  $1.65$  and  $2.0$ , respectively. To clearly see these gaps and the edge states, we enlarge the G-I, -II, and -IV in Figs. 5(b)-(d), respectively.

From Figs. 5(b)-(d), one can see that when the Fermi energy  $\epsilon_f$  lies in the G-I (or -II, -IV), there is only one intersection between  $\epsilon_f$  and the down edge-state energy, which is labeled as point A (B, C) in Fig. 5(b) (5(c), 5(d)). In the left neighboring of the intersection A (B), the down edge-state energy is connected with the lower band. So the winding number of the edge state is  $I_{I(II)} = +1$ . But in the left neighboring of the intersection C, the down edge-state energy is connected with the upper band. The winding number of the edge state is  $I_{IV} = -1$ . By the way, since there is no edge-state energy lies in the Mott gap, there is no intersection between  $\epsilon_f$  and the left edge-state energy when  $\epsilon_f$  lies in the Mott gap, and correspondingly, the winding number is  $I_{III} = 0$ . So, with the topological edge theory, one can easily obtain that when the Fermi energy  $\epsilon_f$  lies in the bulk gaps, the QHC is

$$\sigma_{xy}^{\text{edge}} = \begin{cases} -\frac{e^2}{h} I_I = -\frac{e^2}{h_2}, & \epsilon_f \in \text{G-I} \\ -\frac{e^2}{h} I_{II} = -\frac{e^2}{h}, & \epsilon_f \in \text{G-II} \\ -\frac{e^2}{h} I_{III} = 0, & \epsilon_f \in \text{the Mott gap} \\ -\frac{e^2}{h} I_{IV} = \frac{e^2}{h}, & \epsilon_f \in \text{G-IV} \end{cases} \quad (7)$$

Similar to the discussion in case-I, to check the above results, we also recalculate the HC of the corresponding 2D kagomé lattice *without* boundaries. After a straightforward numerical calculation, one obtains that the Chern numbers are  $-1, 0, 1, 1, 0, -1$  from the lowest to the topmost band. When the Fermi energy  $\epsilon_f$  lies in G-I, only the lowest band is fully filled. So the HC is  $\sigma_{xy}^{\text{I,bulk}} = \frac{e^2}{h} C_1 = -\frac{e^2}{h}$ ; When  $\epsilon_f$  lies in G-II, the lowest two bands are fully occupied,  $\sigma_{xy}^{\text{II,bulk}} = \frac{e^2}{h} (C_1 + C_2) = -\frac{e^2}{h}$ ; When  $\epsilon_f$  lies in the Mott gap,  $\sigma_{xy}^{\text{III,bulk}} = \frac{e^2}{h} \sum_{n=1}^3 C_n = 0$ ; When  $\epsilon_f$  lies in G-IV, the lowest four bands are fully occupied,  $\sigma_{xy}^{\text{IV,bulk}} = \frac{e^2}{h} \sum_{n=1}^4 C_n = \frac{e^2}{h}$ . Comparing with Eq. (7), one can also obtain that  $\sigma_{xy}^{\text{edge}} = \sigma_{xy}^{\text{bulk}}$ . In Fig. 6(b) we plot the HC as a function of the Fermi energy  $\epsilon_f$ . From this figure, one can see  $\sigma_{xy}$  is similar to that in the strong

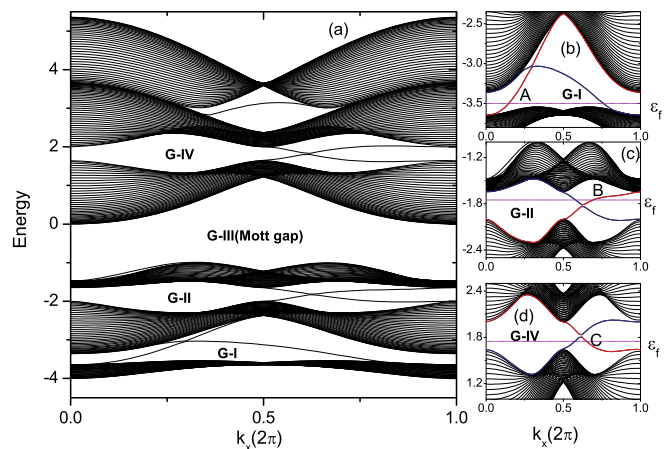


FIG. 5: (Color online) (a) The energy spectrum of 2D kagomé lattice with edges along the  $y$  direction. The parameters are chosen as  $J_0 = 2$ ,  $\theta = \pi/3$ . The shaded areas are energy bands and the lines are the spectrum of the edge states. In this case, there is a Mott gap. Besides that, there are three other energy gaps, which are enlarged in (b), (c) and (d). In (b)-(d), the red and blue lines correspond to the down and up edge-state energies, respectively.

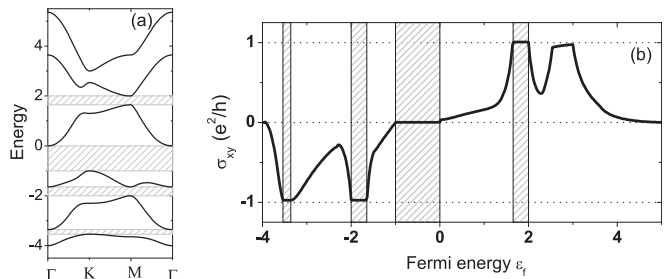


FIG. 6: (a) The energy spectrum of the 2D kagomé lattice without edges. The parameters are same as that in Fig. 5. (b) The Hall conductivity  $\sigma_{xy}$  of this system as a function of the Fermi energy  $\epsilon_f$  at the temperature  $T=0$ . In both figures, the shaded areas are the bulk energy gaps.

Hund's coupling limit. The strength  $J_0$  is more larger, the results more tend to those in the strong Hund's coupling limit. Fig. 6(a) plots the energy spectrum of the system without boundaries.

## IV. SUMMARY

In summary, in this paper we have studied the chiral edge states and the QHC of the 2D kagomé lattice with spin anisotropies included in a general Hund's coupling region. This system is periodic in the  $x$  direction but has two edges in the  $y$  direction. By numerical calculation, we find that both the strength of the Hund's coupling and the spin chirality affect the edges states and the corresponding QHC. Upon varying the chirality

and the strength of the Hund's coupling, two types of phenomena occur, which are distinguished by the critical relation between these two parameters (Eq. (5)). A remarkable difference with the infinite Hund's coupling limit is that there are possibly four edge-state energies in one bulk gap in the case  $J_0 < J_c$ . If the Fermi energy lies in this gap, the HC is quantized as  $\sigma_{xy} = \pm 2 \frac{e^2}{h}$ . We also give the corresponding expression of the QHC without

boundaries within the topological bulk theory. Both two topological expressions give the same QHC.

### Acknowledgments

This work was supported by NSFC under Grants Nos. 10604010 and 60776063.

- 
- [1] K. von Klitzing, G. Dorda and M Pepper, Phys. Rev. Lett. **45**, 494 (1980).
- [2] D.J. Thouless, M. Kohmoto, P. Nightingale and M. den Nijs, Phys. Rev. Lett. **49**, 405 (1982).
- [3] D.J. Thouless, *Topological Quantum Numbers in Nonrelativistic Physics* (World Scientific, Singapore, 1998).
- [4] Y. Hatsugai, Phys. Rev. B **48**, 11851 (1993); Phys. Rev. Lett. **71**, 3697 (1993).
- [5] F.D.M. Haldane, Phys. Rev. Lett. **61**, 2015 (1988).
- [6] K. Ohgushi, S. Murakami, and N. Nagaosa, Phys. Rev. B **62**, R6065 (2000).
- [7] R. Shindou and N. Nagaosa, Phys. Rev. Lett. **87**, 116801 (2001); Z. Wang, P. Zhang, and J. Shi, Phys. Rev. B **76**, 094406 (2007).
- [8] T. Jungwirth, Q. Niu, and A. H. MacDonald, Phys. Rev. Lett. **88**, 207208 (2002).
- [9] Z. Fang, N. Nagaosa, K.S. Takahashi, A. Asamitsu, R. Mathieu, T. Ogasawara, H. Yamada, M. Kawasaki, Y. Tokura, and K. Terakura, Science **302**, 92 (2003).
- [10] Y. Yao, L. Kleinman, A.H. MacDonald, J. Sinova, T. Jungwirth, D.-S. Wang, E. Wang, and Q. Niu, Phys. Rev. Lett. **92**, 037204 (2004).
- [11] P. Matl, N. P. Ong, Y. F. Yan, Y. Q. Li, D. Studebaker, T. Baum, and G. Doubinina, Phys. Rev. B **57**, 10248 (1998).
- [12] S. H. Chun, M. B. Salamon, Y. Lyanda-Geller, P. M. Goldbart, and P. D. Han, Phys. Rev. Lett. **84**, 757 (2000).
- [13] J. Ye, Y. B. Kim, A. J. Millis, B. I. Shraiman, P. Majumdar, and Z. Tešanović, Phys. Rev. Lett. **83**, 3737 (1999).
- [14] Y. Taguchi, Y. Oohara, H. Yoshizawa, N. Nagaosa, and Y. Tokura, Science **291**, 2573 (2001).
- [15] G. Semenoff, Phys. Rev. Lett. **53**, 2449 (1984).
- [16] A. P. Ramirez, Annu. Rev. Mater. Sci. **24**, 453 (1994).
- [17] Z. Wang and P. Zhang, Phys. Rev. B **76**, 064406 (2007).
- [18] B. I. Halperin, Phys. Rev. B **25**, 2185 (1982).
- [19] Z. Wang and P. Zhang, cond-mat/0711.2725v1. to appear in Phys. Rev. B.
- [20] Y. Taguchi and Y. Tokura, Europhys. Lett. **54**, 401 (2001); Y. Taguchi, T. Sasaki, S. Awaji, Y. Iwasa, T. Tayama, T. Sakakibara, S. Iguchi, T. Ito, and Y. Tokura, Phys. Rev. Lett. **90**, 257202 (2003); Y. Yasui, S. Iikubo, H. Harashina, T. Kageyama, M. Ito, M. Sato, and K. Kakurai, J. Phys. Soc. Jpn. **72**, 865 (2003).
- [21] G. Tatara and H. Kawamura, J. Phys. Soc. Jpn. **71**, 2613 (2002).
- [22] M. Taillefumier, B. Canals, C. Lacroix, V. K. Dugaev, and P. Bruno, Phys. Rev. B **74**, 085105 (2006).
- [23] P. G. Harper, Proc. Phys. Soc. London Sect. A **68**, 874 (1955).
- [24] A. Mielke, J. Phys. A **24**, L73(1991); **24**, 3311 (1991); **25**, 4335 (1992).